Archive of Science & Technology
An official Journal of Precious Cornerstone University Ibadan Nigeria
ISSN:0189-3548
Journal Homepage: https://pcujournals.org.ng

Model based Machine Learning Approach to Predict Thermoelectric Figure of Merit

[1]Olayinka A.S., [2]Nwankwo W. and [3]Olayinka T.C.

[1]Department of Physics, Edo University Iyamho. Edo State
[2]Department of Computer Science, Edo University Iyamho, Edo State
[3]Department of Mathematical and Physical Sciences, College of Basic & Applied Sciences, Samuel Adegboyega University, Ogwa, Edo State

ARTICLE INFO

Article history:
Received February 2020
Received in revised form May 2020
Accepted June 2020
Available online June 2020

Keywords:
Thermoelectric
figure of merit
machine learning
uncertainty quantification
DFT
energy.

ABSTRACT

Quest for novel materials with higher thermoelectric figure of merit is on the rise due to global demand for green and renewable energy sources, which is a gradual deviation from the conventional fossil energy sources. Energy problem across the globe is dynamic and it varies from one clime to another. In addressing the quantum demand for these new materials, experimentalists are limited to certain domain of materials classes like chalcogenides, skutterudites, and Zintl phases in their search for newer materials due to experimental constraints. Computational data from theorist usually guide the chemistry of experimentalist in their search and synthesis of new materials. However, Ab initio computation of thermoelectric properties remains herculean and computationally expensive. We present a machine learning (ML) model to predict thermoelectric figure of merit, ZT from chemical formula. Datasets from citrine and materials project were obtained using Application Program Interface (API). The Standard Error in the estimate of Root mean squared error (RMSE) was 0.0135 and Uncertainty calibration was recorded to be 0.662 translating to percentage error of 2.6% in calibration uncertainty. The ML model was used in the prediction of thermoelectric figure of merit for several compound and the results are presented with their probability density.

*Corresponding author.
E-mail address: solayinkaa@gmail.com / akinola.olayinka@edouniversity.edu.ng

https://doi.org/10.xxx.

1.0 Introduction

Material research is central to technological revolution and advancement. Over the years, the material industry has witness dynamics in discovery of new materials for applications in various areas of human endeavours. Experimental research in material research are usually tedious and expensive while Density Functional Theory (DFT), which has contributed in no small measure to revolution in material research can be computationally demanding and costly. DFT also has limitations in accurate representation of experimental results (Adetunji et al., 2016; Curtarolo et al., 2013; Olayinka, Adetunji, et al., 2019; Olayinka, Idiodi, et al., 2019; Zhang & Wang, 2011). Quest for better and efficient materials in several

applications like photovoltaic and thermoelectric has heralded a new era in material research with the deployment of Artificial Intelligence (AI), Machine Learning (ML) and Deep Learning (DL) algorithms to material discovery. The application of AI, ML and DL in material research is an evolving area of research (Iwasaki et al., 2019; Liu et al., 2017; Pilania et al., 2013; Raccuglia et al., 2016; Ramprasad et al., 2017). The success of ML and DL algorithms in material research is predicated on quantum of experimental or theoretical datasets repository. ML models are created based on learning from datasets repository which eventually leads to discovery of newer materials for various applications. Crystal structure, band gaps, entropies predictions as well as new materials discovery for applications in metallic glasses and organic flow battery electrolytes are some of the exploits recorded so far in ML materials research (Castelli et al., 2012; Isayev et al., 2017; Jain & Bligaard, 2018; Kim et al., 2017; Legrain et al., 2017; Lu et al., 2018; Meredig et al., 2014; Ren et al., 2018).

Thermoelectric materials enable the conversion of heat energy into electricity. Usually, heat energy in most system is wasted as in automobile engine where a greater percentage of heat generated by the engine is released to the atmosphere. The release of the heat to the atmosphere could be contributing factor to global warming and greenhouse effect. Discovery of more efficient, flexible and cost-effective materials can drive innovations that will lead to thermoelectric generators which is capable converting heat to useful electricity. Conversion of heat to electricity at solid state level has merits in terms of reliability, miniaturization, flexibility and cost efficiency (Dresselhaus et al., 2007; Fang et al., 2018; Zhu et al., 2018, 2019).

In this work, we create a model through experimental design to predict materials with better thermoelectric figure of merit (ZT).

2.0 Methodology

In this section, we present the theoretical formulation for probing thermoelectric properties of materials as well as computational methodology adopted in the experimental design for predicting thermoelectric figure of merit.

2.1 Theoretical Formulation for Thermoelectric Properties

Thermoelectric properties of materials are characterized by the dimensionless quantity known as the thermoelectric figures of merit (ZT), given as:

$$ZT = \frac{\sigma S^2}{\kappa} T \qquad (1)$$

where σ is the electrical conductivity, S is the Seebeck coefficient, T is the temperature while κ is the thermal conductivity.

Thermal conductivity, κ can further be defined as

$$\kappa = \kappa_{ph} + \kappa_e \qquad (2)$$

where $\kappa_{ph}$and $\kappa_e$are phonon and electronic components of thermal conductivity respectively.

Seebeck coefficient of a material quantifies the ratio of induced thermoelectric voltage to temperature difference across the material, as a consequence of the Seebeck effect. Seebeck coefficient is measures in volts per kelvin or microvolts per kelvin. Materials with better thermoelectric properties are those with higher value of ZT and they are potential material for thermoelectric applications. Equation 1 shows that higher value of electrical conductivity and Seebeck coefficient will yield higher value of figure of merit

while lower value of thermal conductivity corresponds to low figure of merit. Maximization of the power factor $(\sigma S^2)$with or without minimization of thermal conductivity $(\kappa_{ph} + \kappa_e)$can give rise to higher thermoelectric figure of merit, ZT. Though this might be difficult experimentally due to the coupling of transport coefficients. Higher ZT value is a desirable feature. Though, electrical conductivity, Seebeck coefficient and thermal conductivity are closely correlated, material informatics is considered as a better alternative in quest for materials with higher figure of merit without the hassle of rigorous experiment and computationally expensive simulation while predicting properties of materials.

Efficiency of the thermoelectric materials ability to convert heat to electricity is correlated by the Carnot efficiency, η and the figure-of-merit, ZT of the material:

$$\eta = \left(\frac{T_{hot} - T_{cold}}{T_{hot}}\right)\left(\frac{\sqrt{1+ZT_m}-1}{\sqrt{1+ZT_m}+\left(\frac{T_{cold}}{T_{hot}}\right)}\right) \qquad (3)$$

where T_{hot}, $T_{cold}$and $T_m$are hot-side temperature, cold-side temperature and mean temperature respectively. [18]

2.2 Dataset Description and Preparation

Thermoelectric dataset of Gaultois *et al* (Gaultois et al., 2013) as reposited in Citrine Informatics Artificial Intelligence (AI) powered materials data platform (https://citrination.com). The original thermoelectric dataset contains a collection of thermoelectric properties, such as thermal and electrical conductivities, for various thermoelectric materials as well as thermoelectric figure of merit. Dataset contains experimentally computed thermoelectric figure of merit at 300K, 400K, 700K and 1000K. For this work, thermoelectric dataset measured at 300K were extracted and used in model building as well as machine learning training. The dataset consists of 195 figure of merit (ZT) measured experimentally for different inorganic compounds at 300K. In developing for the model, quality of the training dataset was ensured by using data filtering approach to eliminate noise from the dataset.

2.3 Technical Procedure

In predicting the thermoelectric figure of merit, python 3.6 distribution by Anaconda (Anaconda Inc., 2019) was used in data preparation as well as python interface to Citrine Informatics Artificial Intelligence (AI) powered materials data platform (https://citrination.com). Python interface with citrination platform was achieved through Application Programming Interface (API) provided by citrination as illustrated in Fig. 1. Datasets uploaded to citrination is searchable, shareable, and accessible for machine learning. Using the dataview option from the citrination platform, thermoelectric figure of merit for novel materials are predicted. The Lolo estimator in the Citrine's open source machine-learning library was used with Ensemble of non-linear estimators. Jackknife method of uncertainty estimation was used with three-fold cross-validation. Number of estimators used were 145 with a maximum tree depth of 30.

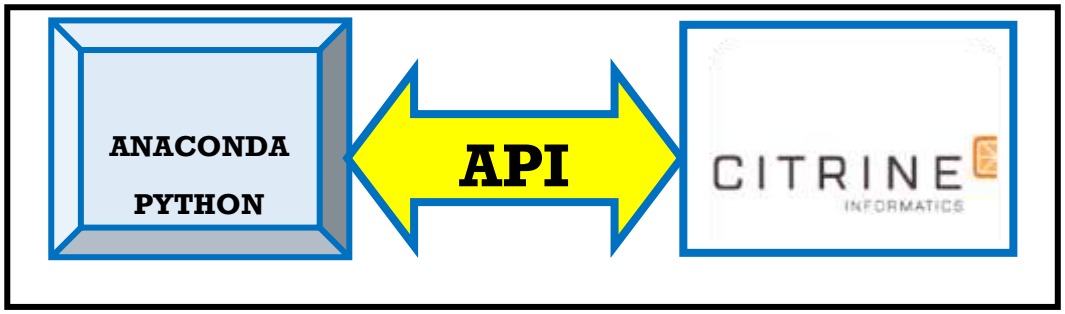

Figure 1: ML Model for Python Interface with Citrination Platform

3.0 Results

3.1 Machine Learning Model Training and Performance

Dataset described in section 2.2 was used as the training dataset to train the machine learning model for predicting thermoelectric figure of merit. Fig 2 shows the number of training examples and a distribution of thermoelectric figure of merit.

In training the model, important features from the chemical formula, used in the training of the model were ranked by their order of importance. Importance scores added up to 1 and these represent the contributions of various features to the overall model performance. Fig. 3 shows the Pearson Correlation for the model training performance for individual contributors. Pearson Correlation is a statistical measure of linear correlation between binary variables. Pearson Correlation Coefficient ranges between +1 and −1 with +1 as the total positive linear correlation while −1 is total negative linear correlation and Pearson Correlation Coefficient value of 0 indicates zero linear correlation between the binary variables. From Fig. 3, the Pearson Correlation Coefficient for the of Valence electron density for formula is 0.447 which is the highest Coefficient. Other top Correlation Coefficient are 0.435 and 0.407 for Min atomic radius plus max electronegativity difference for formula and mean of Trouton's Ratio for formula respectively. Lowest coefficient as shown in the figure are 0.225 for the Maximum weight fraction for formula and 0.218 for Minimum weight fraction for formula.

On the other hand, the distance correlation, which measures the dependency between two paired random vectors of arbitrary, not necessarily equal, dimension. When random vectors are independent, the distance correlation coefficient will be zero. In essence, distance correlation measures both linear and nonlinear association between two random variables or random vectors. Distance correlation is different from the Pearson's correlation because the latter only measures linear association between two random variables. Fig. 4 shows the distance correlation for our model's performance. Minimum atomic radius plus max electronegativity difference for formula, has distance correlation coefficient of 0.513 which is the highest coefficient. This is closely followed by the mean of Row in periodic table for formula and Maximum radius ratio for formula with distance coefficients of 0.491 and 0.477 respectively. Least distance coefficients for the mean of Radius of d orbitals for formula was and 0.405.

On Citrination Platform, feature that are crucial as inputs to machine learning model for predicting thermoelectric figure of merit are the mean of Total number of valence electrons for formula, the mean of Number of d valence electrons for formula and the mean of DFT energy density for formula with 26%, 12%, and 7% contribution to model performance respectively. The mean of Non-dimensional work function for formula, has 5% contribution while mean of Valence electron density for formula and mean of Elemental melting temperature for formula, contributed 4% each. For mean of Elemental bulk modulus for formula, a performance contribution to the model was 3%. Others such has mean of Radius of d orbitals for formula, Maximum weight fraction for formula, mean of Moduli sum for formula, Minimum atomic radius plus max electronegativity difference for formula, mean of Row in periodic table for formula, mean of Liquid range for formula, mean of Number of valence electrons for formula, mean of Number of p valence electrons for formula contributed 2% each to the model performance.

A performance contribution of 1% was recorded for mean of Elemental polarizability for formula, mean of Ratio of Electron Affinity to Electronegativity for formula, mean of Elemental crystal structure (space group) for formula, mean of Elastic Poisson Ratio for formula, Formula weight for formula, mean of Elemental atomic volume for formula, Minimum weight fraction for formula, Maximum radius difference for formula, mean of Shear Modulus Melting Temp Product for formula, Maximum radius ratio for formula and mean of Elemental density for formula.

Maximum electronegativity difference, mean of Radius of s orbitals, mean of Packing density, mean of Miracle Ratio, mean of Elemental work function, mean of Ionization Affinity Ratio, Minimum atomic fraction, mean of DFT volume ratio, and mean of Mendeleev number for formula also has percentage performance contribution of 1%.

Mean of Radius of p orbitals mean of Trouton's Ratio, mean of Conduction ionization energy, Number of elements, Non-dimensional liquid range, mean of Total number of unfilled valence electrons and maximum atomic fraction for formula have no contribution to the model performance.

Root mean squared error (RMSE) for model testing on the training dataset was 0.0907 as against 0.0 expected for a perfect model while the Standard Error in the estimate of RMSE was 0.0135 where a perfect estimator should have a Standard Error value of 0.0. Uncertainty calibration which is defined as the fraction of actual values within the prediction error bars was recorded to be 0.662 while a perfectly calibrated uncertainty is 0.68. Percentage error in calibration uncertainty was computed as 2.6%.

For uncertainty calibration, the root mean square of standardized errors (RMSSE) was 1.45 while the expected was 1.0 for a perfectly calibrated. Fig. 5 shows the Model Performance for Actual and Predicted thermoelectric figure of merit while Fig. 6 shows the Probability Density Distribution of Standard residuals for ideal and actual values. Fig 7 shows the T-distributed Stochastic Neighbor Embedding (t-SNE) distribution for the training dataset. T-SNE is a nonlinear dimensionality reduction method and a machine learning algorithm for visualization (Van Der Maaten & Hinton, 2008).

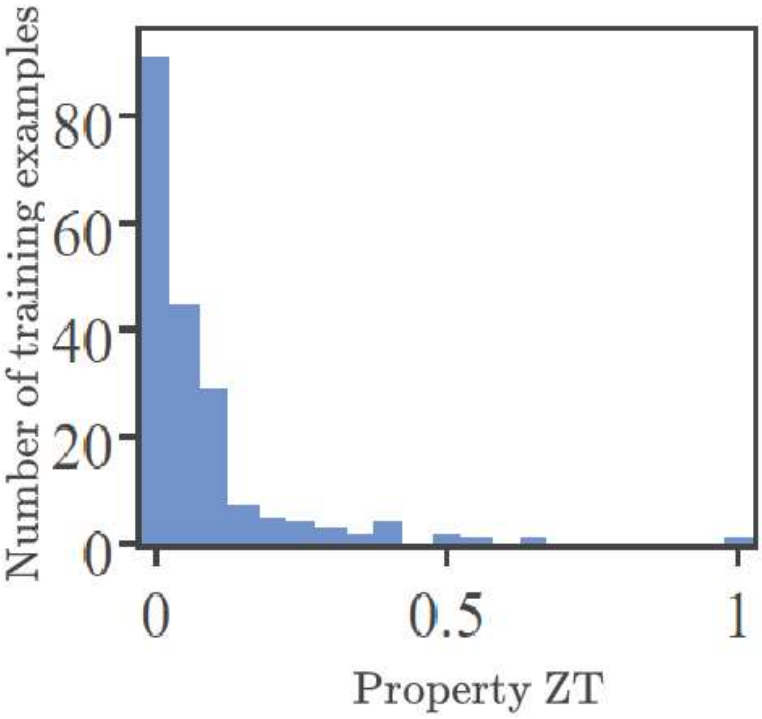

Fig. 2: Distribution of thermoelectric figure of merit for Training Dataset

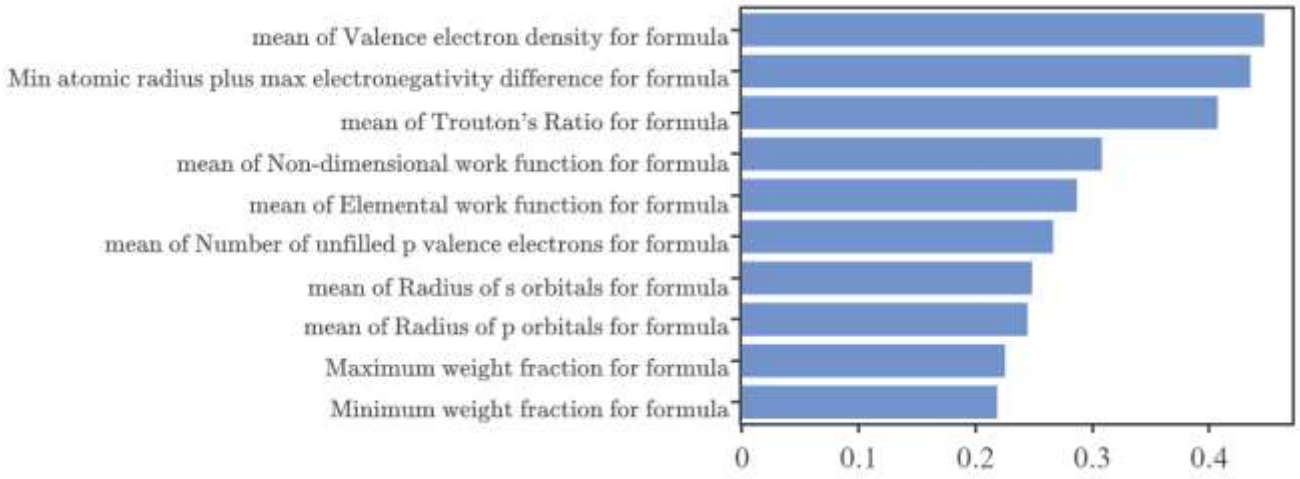

Fig. 3: Pearson Correlation for Model's Performance

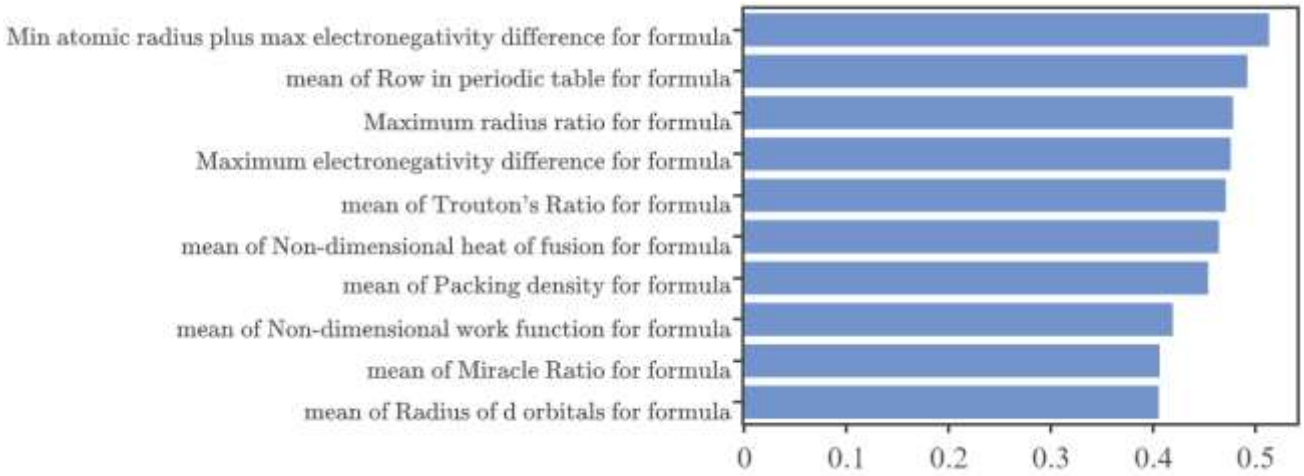

Fig. 4: Distance Correlation for Model's Performance

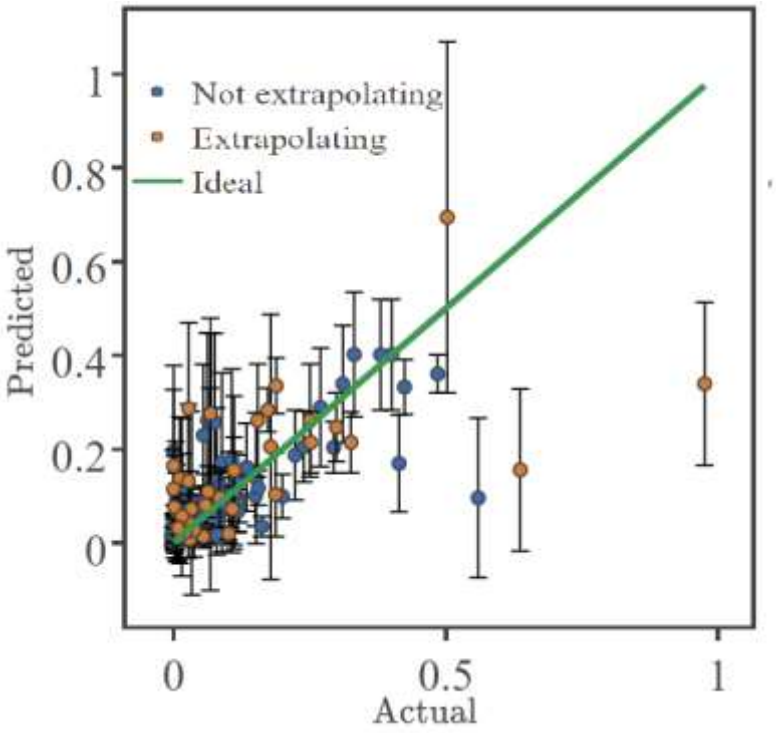

Fig. 5: Model Performance for Actual and Predicted

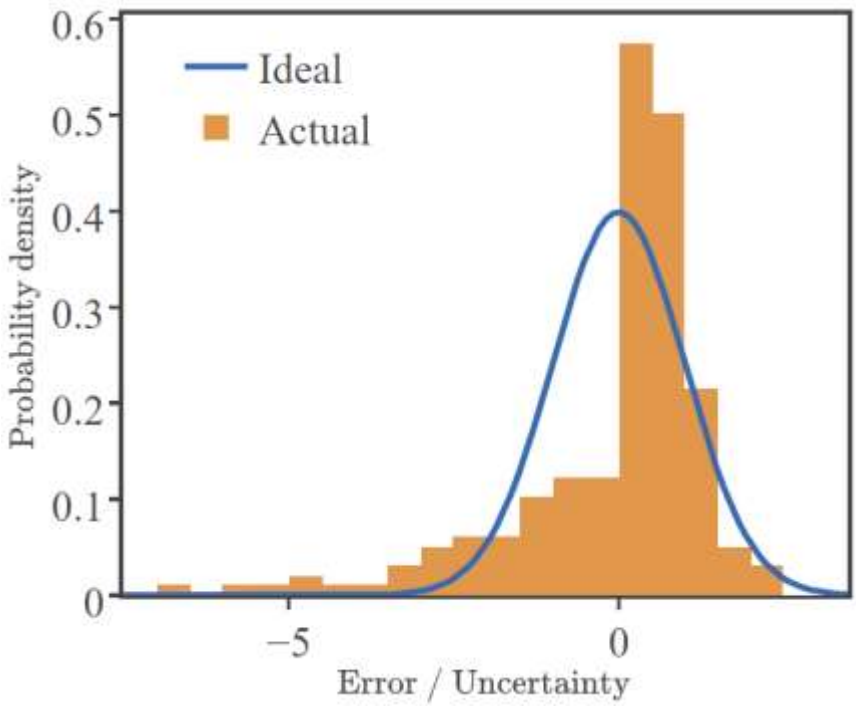

Fig. 6: Probability Density Distribution of Standards

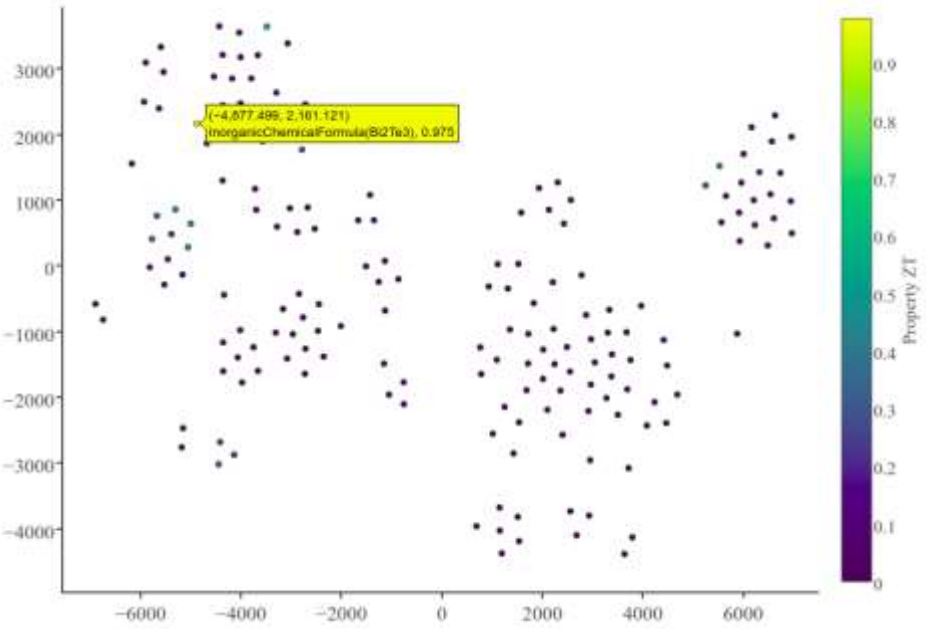

Fig. 7: The t-SNE projection

3.2 Predicted Thermoelectric Figure of Merit

Fig 8 and fig. 9 shows predicted thermoelectric figure of merit for various inorganic compound at 300K. Thermoelectric figure of merits predicted and their tolerance for Half Heusler alloys as well as their probability distribution are shown in fig 8. Half Heusler HfNiX (X=As, Ga, Ge, Pb, Si, Sn) alloys were explored using the machine learning model and the predicted thermoelectric figure of merits for each strand of the alloys are presented in table 2. HfNiPb and HfNiGe have approximately the highest predicted

thermoelectric figure of merit of 0.24 while HfNiSi has the lowest value of 0.09. Bismuth base compounds predicted are also shown in table 1, Bi_2Te_3 has the highest predicted thermoelectric figure of merit value of 0.65± 0.28, closely followed by 0.52 ± 0.31 for $Bi_{1.9}Sb_{0.1}Te_3$. Predicted thermoelectric figure of merit for ZrRuTe was 0.11 at 300K which compares well with the 0.13 measured by Keshri & Medhi (2020). For ScNiSb we predicted a 0.08 while 0.1 was measured by experimentalist (Synoradzki et al., 2019). It may be possible to predict higher thermoelectric figure of merit at higher temperature for thermometric materials. Probability distribution for the predicted thermoelectric figure of merit for Half Heusler HfNiX (X=As, Ga, Ge, Pb, Si, Sn) alloys are shown in fig. 8 while that of Bismuth based compounds are shown in fig 9. Fig. 10 shows the predicted thermoelectric figure of merit for other compounds and their probability distribution.

Table 1: Predicted Thermoelectric Figure of Merit

Compound	**Predicted Figure of Merit @ 300K**	**Other Works Figure of Merit**	**References**
ZrRuTe	0.11	0.13 @ 800K	(Keshri & Medhi, 2020)
p-doped ZrRuTe	-	0.2 @ 800K	
ScNiSb	0.08	0.1 @ 810K	(Synoradzki et al., 2019)
HfNiAs	0.22	-	-
HfNiGa	0.23	-	-
HfNiGe	0.24	-	-
HfNiPb	0.24	-	-
HfNiSi	0.09	-	-
HfNiSn	0.22	-	-
$Bi_{1.5}Sb_{0.5}Te_3$	0.47		
$Bi_{1.5}Sb_{0.5}Te_3$ (multilayered Thin film)	-	1.28	Tan et al., 2013)
Bi1.5Sb0.5Te3 (nanopillar)	-	1.61	(Tan et al., 2018)
$Bi_{1.8}Sb_{0.2}Te_3$	0.47	-	-
$Bi_{1.9}Sb_{0.1}Te_3$	0.52	-	-
Bi_2Se_3	0.21	-	-
Bi_2Te_2Se	0.36	-	-
Bi_2Te_3	0.65	-	-
$BiTe_3$	0.42	-	-
$BaBiTe_3$	0.45	-	-
Cs_2Te_3	0.16	-	-
$SbTe_3$	0.42	-	-
$AsTe_3$	0.43	-	-
$Cu_2ZnSnSe_4$	0.21	-	-

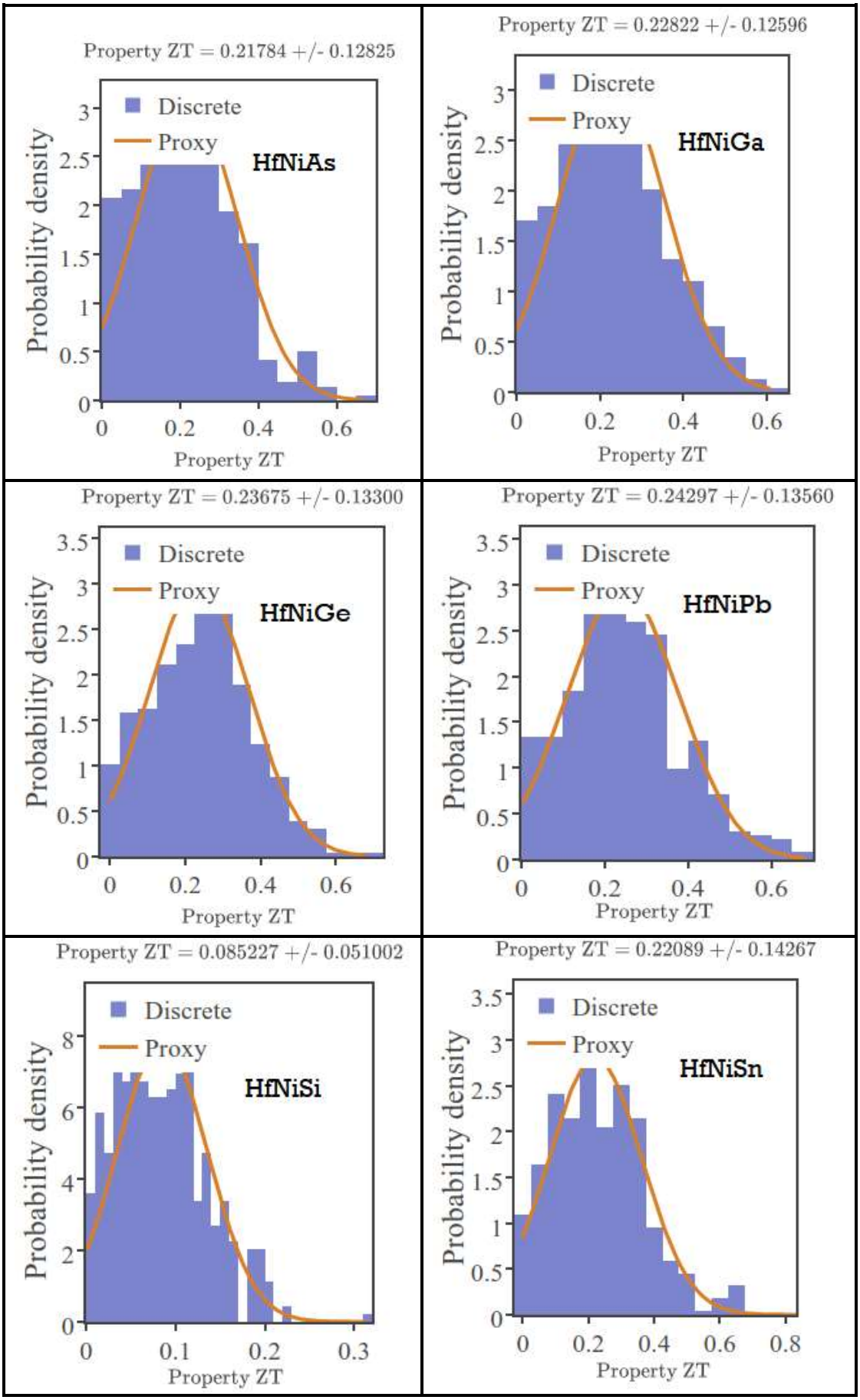

Fig 8: Predicted Thermoelectric figure of merit for 6 Husler Alloys

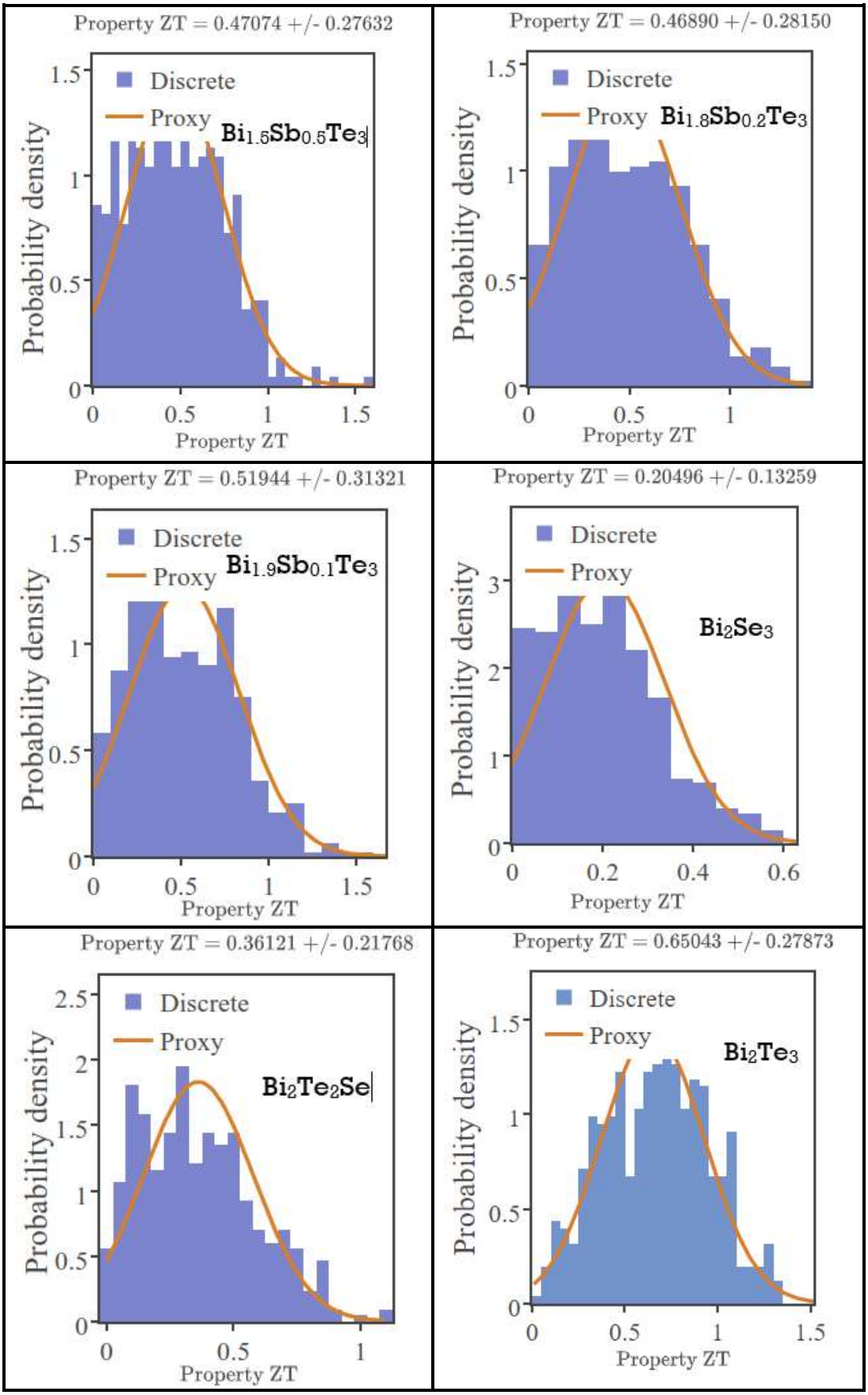

Fig 9: Predicted Thermoelectric figure of merit for Bismuth base Compounds

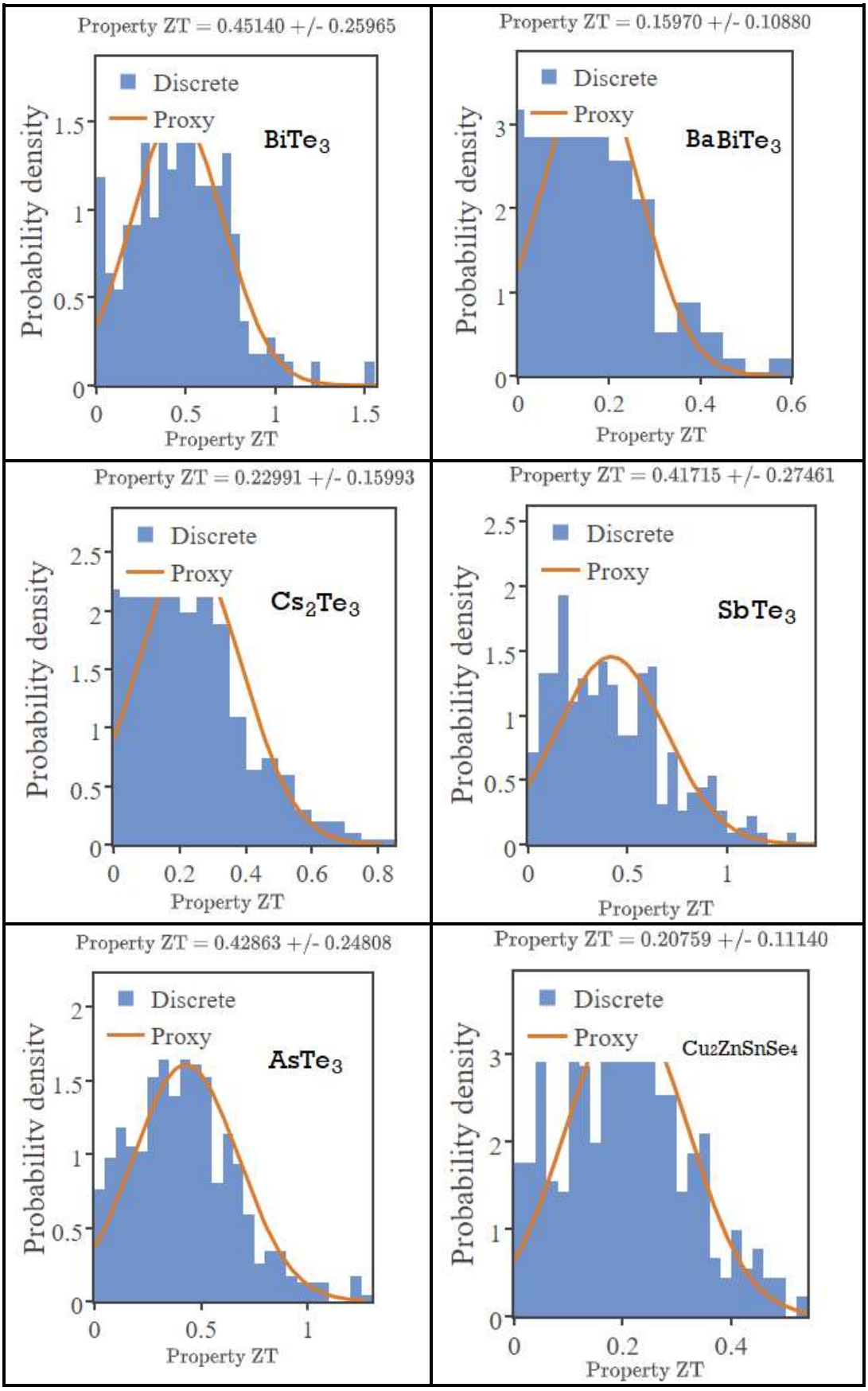

Fig 10: Predicted Thermoelectric figure of merit for Other Compounds

4.0 Conclusion

Machine learning model has been developed using python and citrination Artificial intelligent material platform. The model was trained using experimental dataset of thermoelectric figure of merit calculated at 300K for various inorganic compounds. The model accuracies, performance and validation were reported and discussed. The model was applied to predict thermoelectric figure of merit for several inorganic compounds. The probability density for predicted compound were presented and discussed. The predicted results for known thermoelectric figure of merits compares favourably with experimental results.. The model is available online on the citrination platform as UCSB@300K-DataView for predicting thermoelectric figure of merit for unknown inorganic compounds.

Acknowledgements
One of the authors (A.S. Olayinka) is indebted to Simons Trust Imbizo Follow Up Grant (STIFUG) for partial support towards this research.

Conflict of Interest
The authors declare no conflict of interest.

References

Adetunji, B. I., Olayinka, A. S., Fashae, J. B., & Ozebo, V. C. (2016). Ab initio investigation of the electronic, lattice dynamic and thermodynamic properties of ScCd intermetallic alloy. *International Journal of Modern Physics B*, *30*(24). https://doi.org/10.1142/S0217979216501757

Anaconda Inc. (2019). *Home - Anaconda*. 2019-05-19.

Castelli, I. E., Olsen, T., Datta, S., Landis, D. D., Dahl, S., Thygesen, K. S., & Jacobsen, K. W. (2012). Computational screening of perovskite metal oxides for optimal solar light capture. *Energy and Environmental Science*. https://doi.org/10.1039/c1ee02717d

Curtarolo, S., Hart, G. L. W., Nardelli, M. B., Mingo, N., Sanvito, S., & Levy, O. (2013). The high-throughput highway to computational materials design. *Nature Materials*. https://doi.org/10.1038/nmat3568

Dresselhaus, M. S., Chen, G., Tang, M. Y., Yang, R., Lee, H., Wang, D., Ren, Z., Fleurial, J. P., & Gogna, P. (2007). New directions for low-dimensional thermoelectric materials. *Advanced Materials*. https://doi.org/10.1002/adma.200600527

Fang, T., Zhao, X., & Zhu, T. (2018). Band structures and transport properties of high-performance half-heusler thermoelectric materials by first principles. In *Materials*. https://doi.org/10.3390/ma11050847

Gaultois, M. W., Sparks, T. D., Borg, C. K. H., Seshadri, R., Bonificio, W. D., & Clarke, D. R. (2013). Data-driven review of thermoelectric materials: Performance and resource onsiderations. In *Chemistry of Materials*. https://doi.org/10.1021/cm400893e

Isayev, O., Oses, C., Toher, C., Gossett, E., Curtarolo, S., & Tropsha, A. (2017). Universal fragment descriptors for predicting properties of inorganic crystals. In *Nature Communications*. https://doi.org/10.1038/ncomms15679

Iwasaki, Y., Takeuchi, I., Stanev, V., Kusne, A. G., Ishida, M., Kirihara, A., Ihara, K., Sawada, R., Terashima, K., Someya, H., Uchida, K. ichi, Saitoh, E., & Yorozu, S. (2019). Machine-learning guided discovery of a new thermoelectric material. *Scientific Reports*. https://doi.org/10.1038/s41598-019-39278-z

Jain, A., & Bligaard, T. (2018). Atomic-position independent descriptor for machine learning of material properties. *Physical Review B*. https://doi.org/10.1103/PhysRevB.98.214112

Keshri, S. P., & Medhi, A. (2020). Intrinsically high thermoelectric figure of merit of half-Heusler ZrRuTe. *Journal of Physics: Condensed Matter*. http://iopscience.iop.org/10.1088/1361-648X/ab9d49

Kim, S., Jinich, A., & Aspuru-Guzik, A. (2017). MultiDK: A Multiple Descriptor Multiple Kernel Approach for Molecular Discovery and Its Application to Organic Flow Battery Electrolytes. *Journal*

of Chemical Information and Modeling. https://doi.org/10.1021/acs.jcim.6b00332

Legrain, F., Carrete, J., Van Roekeghem, A., Curtarolo, S., & Mingo, N. (2017). How Chemical Composition Alone Can Predict Vibrational Free Energies and Entropies of Solids. *Chemistry of Materials*. https://doi.org/10.1021/acs.chemmater.7b00789

Liu, Y., Zhao, T., Ju, W., Shi, S., Shi, S., & Shi, S. (2017). Materials discovery and design using machine learning. In *Journal of Materiomics*. https://doi.org/10.1016/j.jmat.2017.08.002

Lu, S., Zhou, Q., Ouyang, Y., Guo, Y., Li, Q., & Wang, J. (2018). Accelerated discovery of stable lead-free hybrid organic-inorganic perovskites via machine learning. *Nature Communications*. https://doi.org/10.1038/s41467-018-05761-w

Meredig, B., Agrawal, A., Kirklin, S., Saal, J. E., Doak, J. W., Thompson, A., Zhang, K., Choudhary, A., & Wolverton, C. (2014). Combinatorial screening for new materials in unconstrained composition space with machine learning. *Physical Review B - Condensed Matter and Materials Physics*. https://doi.org/10.1103/PhysRevB.89.094104

Olayinka, A. S., Adetunji, B. I., Idiodi, J. O. A., & Aghemelon, U. (2019). Ab initio study of electronic and optical properties of nitrogen-doped rutile TiO2. *International Journal of Modern Physics B*, *33*(06), 1950036.

Olayinka, A. S., Idiodi, O. A. J., & Nwankwo, W. (2019). Electronics and Optical Properties of Nitrogen Doped Anatase for Solar Application. In *Covenant Journal of Physical & Life Sciences (CJPL)*.

Pilania, G., Wang, C., Jiang, X., Rajasekaran, S., & Ramprasad, R. (2013). Accelerating materials property predictions using machine learning. *Scientific Reports*. https://doi.org/10.1038/srep02810

Raccuglia, P., Elbert, K. C., Adler, P. D. F., Falk, C., Wenny, M. B., Mollo, A., Zeller, M., Friedler, S. A., Schrier, J., & Norquist, A. J. (2016). Machine-learning-assisted materials discovery using failed experiments. *Nature*. https://doi.org/10.1038/nature17439

Ramprasad, R., Batra, R., Pilania, G., Mannodi-Kanakkithodi, A., & Kim, C. (2017). Machine learning in materials informatics: Recent applications and prospects. In *npj Computational Materials*. https://doi.org/10.1038/s41524-017-0056-5

Ren, F., Ward, L., Williams, T., Laws, K. J., Wolverton, C., Hattrick-Simpers, J., & Mehta, A. (2018). Accelerated discovery of metallic glasses through iteration of machine learning and high-throughput experiments. *Science Advances*. https://doi.org/10.1126/sciadv.aaq1566

Synoradzki, K., Ciesielski, K., Veremchuk, I., Borrmann, H., Skokowski, P., Szymański, D., Grin, Y., & Kaczorowski, D. (2019). Thermal and electronic transport properties of the half-heusler phase ScNiSb. *Materials*. https://doi.org/10.3390/MA12101723

Tan, M., Hao, Y., Deng, Y., Yan, D., & Wu, Z. (2018). Tilt-structure and high-performance of hierarchical Bi1.5Sb0.5Te3 nanopillar arrays. *Scientific Reports*. https://doi.org/10.1038/s41598-018-24872-4

Van Der Maaten, L., & Hinton, G. (2008). Visualizing data using t-SNE. *Journal of Machine Learning Research*.

Zhang, Y. G., & Wang, Y. X. (2011). Calculations show improved photoelectrochemical performance for N, Ce, and Ce+ N doped anatase TiO2. *Journal of Applied Physics*, *110*(3), 33519.

Zhu, H., He, R., Mao, J., Zhu, Q., Li, C., Sun, J., Ren, W., Wang, Y., Liu, Z., Tang, Z., Sotnikov, A., Wang, Z., Broido, D., Singh, D. J., Chen, G., Nielsch, K., & Ren, Z. (2018). Discovery of ZrCoBi based half Heuslers with high thermoelectric conversion efficiency. *Nature Communications*. https://doi.org/10.1038/s41467-018-04958-3

Zhu, H., Mao, J., Li, Y., Sun, J., Wang, Y., Zhu, Q., Li, G., Song, Q., Zhou, J., Fu, Y., He, R., Tong, T., Liu, Z., Ren, W., You, L., Wang, Z., Luo, J., Sotnikov, A., Bao, J., … Ren, Z. (2019). Discovery of TaFeSb-based half-Heuslers with high thermoelectric performance. *Nature Communications*. https://doi.org/10.1038/s41467-018-08223-5